

Accepted Manuscript

Research papers

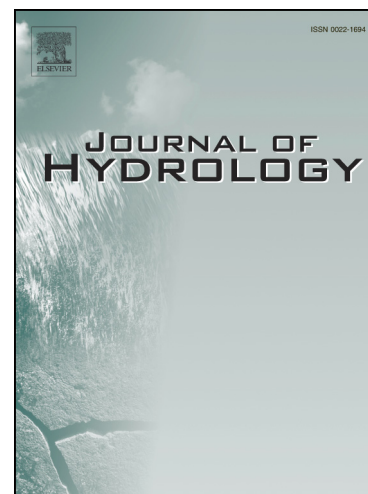
Assessing acid rain and climate effects on the temporal variation of dissolved organic matter in the unsaturated zone of a karstic system from southern China

Jin Liao, Chaoyong Hu, Miao Wang, Xiuli Li, Jiaoyang Ruan, Ying Zhu, Ian J. Fairchild, Adam Hartland

PII: S0022-1694(17)30808-9
DOI: <https://doi.org/10.1016/j.jhydrol.2017.11.043>
Reference: HYDROL 22401

To appear in: *Journal of Hydrology*

Received Date: 17 February 2017
Revised Date: 10 August 2017
Accepted Date: 23 November 2017



Please cite this article as: Liao, J., Hu, C., Wang, M., Li, X., Ruan, J., Zhu, Y., Fairchild, I.J., Hartland, A., Assessing acid rain and climate effects on the temporal variation of dissolved organic matter in the unsaturated zone of a karstic system from southern China, *Journal of Hydrology* (2017), doi: <https://doi.org/10.1016/j.jhydrol.2017.11.043>

This is a PDF file of an unedited manuscript that has been accepted for publication. As a service to our customers we are providing this early version of the manuscript. The manuscript will undergo copyediting, typesetting, and review of the resulting proof before it is published in its final form. Please note that during the production process errors may be discovered which could affect the content, and all legal disclaimers that apply to the journal pertain.

Assessing acid rain and climate effects on the temporal variation of dissolved organic matter in the unsaturated zone of a karstic system from southern China

Jin Liao^{a,b}, Chaoyong Hu^{a,b*}, Miao Wang^c, Xiuli Li^a, Jiaoyang Ruan^a, Ying Zhu^d, Ian J. Fairchild^e, Adam Hartland^f

^a State Key Laboratory of Biogeology and Environmental Geology, China University of Geosciences, Wuhan, 430074, China

^b School of Earth Sciences, China University of Geosciences, Wuhan, 430074, China

^c Wuhan Regional Climate Center, China Meteorological Administration, 430074, China

^d Changsha Uranium Geology Research Institute, China National Nuclear Cooperation, Changsha, 410007, China

^e School of Geography, Earth and Environmental Sciences, University of Birmingham, Birmingham, B15 2TT, UK

^f Environmental Research Institute, School of Science, Faculty of Science and Engineering, University of Waikato, Hamilton, New Zealand

* Corresponding author. Tel: +86 27 67883933

E-mail address: chyhu@cug.edu.cn (C. Hu)

Abstract: Acid rain has the potential to significantly impact the quantity and quality of dissolved organic matter (DOM) leached from soil to groundwater. Yet, to date, the effects of acid rain have not been investigated in karstic systems, which are expected to strongly buffer the pH of atmospheric rainfall. This study presents a nine-year DOM fluorescence dataset from a karst unsaturated zone collected from two drip sites (HS4, HS6) in Heshang Cave, southern China between 2005 and 2014. Cross-correlograms show that fluorescence intensity of

both dripwaters lagged behind rainfall by ~1 year (~11 months lag for HS4, and ~13 months for HS6), whereas drip rates responded quite quickly to rainfall (0 months lag for HS4, and ~3 months for HS6), based on optimal correlation coefficients. The rapid response of drip rates to rainfall is related to the change of reservoir head pressure in summer, associated with higher rainfall. In winter, low rainfall has a limited effect on head pressure, and drip rates gradually slow to a constant value associated with base flow from the overlying reservoir- this effect being most evident on inter-annual timescales ($R^2 = 0.80$ for HS4 and $R^2 = 0.86$ for HS6, $n = 9$, $p < 0.01$). We ascribed the ~1 year lag of fluorescence intensity to the effect of the soil moisture deficit and the karst process on delaying water and solute transport. After eliminating the one year lag, the congruent seasonal pacing and amplitude between fluorescence intensity and rainfall observed suggests that the seasonality of fluorescence intensity was mainly controlled by the monsoonal rains which can govern the output of DOM from the soil, as well as the residence time of water in the unsaturated zone. On inter-annual timescales, a robust linear relationship between fluorescence intensity and annual (effective) precipitation amount ($R^2 = 0.86$ for HS4 and $R^2 = 0.77$ for HS6, $n = 9$, $p < 0.01$) was identified, implying that annual (effective) precipitation is the main determinant of DOM concentration in the aquifer. Conversely, the insensitivity of fluorescence intensity and fluorescence wavelength maxima to variations in the pH of local rainfall suggests that acid rain over the study period (~pH 5.6 to ~4.5) had no discernable effect on the quantity and quality of DOM in karst soil and soil solution, likely being strongly buffered by soil carbonates. Therefore, despite large increases in anthropogenic acid rain in recent Chinese history, hydrologic forcing is the predominant factor driving variations in DOM in karst aquifers.

Keywords: Karst groundwater; Unsaturated Zone; Dissolved Organic Matter; Fluorescence; Climate change; Acid rain

1. Introduction

Groundwater is a major water resource for human societies and is of increasing importance because of overuse and serious contamination of surface fresh water in some countries (Shen et al., 2015; McCormack et al., 2016). This situation is much worse in the karst aquifers of southern China, which are characterized by a high vulnerability to contamination (Ford and Williams, 2007; Jiang et al., 2009). Protecting the quality of karst groundwater is therefore a key challenge for this region.

Natural organic matter (NOM) in groundwater mainly derives from the soil zone, and is a potential contaminant in groundwater because of the ability of NOM to transport contaminants (Ritson et al., 2014; Schipperski et al., 2015; Graham et al., 2015; Hartmann et al., 2016). NOM can also transform into carcinogenic disinfection by-products during ozonation and chlorination in drinking water treatment processes and this becomes relevant when considering groundwater for use as a potable water resource (Papageorgiou et al., 2016). Moreover, the composition of NOM also influences groundwater quality. NOM can be operationally divided into particle organic matter (POM; > around 0.45 μm) and dissolved organic matter (DOM; < around 0.45 μm) based on typical filtration protocols (e.g. Hartland et al., 2011; Andrade-Eiroa et al., 2013). DOM can be further classified into colloidal (diameter defined between 1 nm and 1 μm generally) (e.g. Lead and Wilkinson, 2006; Hartland et al., 2012), hydrophobic (characterized by high aromaticity and molecular weight, e.g. containing a higher proportion of phenolic groups), and hydrophilic fractions (characterized by low aromaticity and molecular weight, e.g. containing more carboxylic groups) (e.g. Thurman, 1985; Senesi et al., 1991; Tipping and Woof, 1991; Ekström et al., 2011). Due to the specific surface chemistry and high stability of DOM, it can directly facilitate the solubility and transport of contaminants, such as toxic metals between surface environments and aquifers, ultimately

deteriorating groundwater quality (e.g. Hartland et al., 2012, 2014, 2015; Yang et al., 2012; Rutledge et al., 2014; Klučáková and Kalina, 2015). It is well understood that DOM accounts for a large fraction of NOM in groundwater (up to 90%), and can be considered synonymous with NOM (e.g. Thurman, 1985; Andrade-Eiroa et al., 2013).

Acid rain ($\text{pH} < 5.6$) has been proposed to strongly influence the quantity and quality of DOM in soil solution through changes in the ionization of constituent organic molecules (Evans et al., 2005; SanClements et al., 2012).

Widespread studies of DOM increases in natural waters from across Europe and North America have been reported over the last two decades. These have been largely ascribed to the long-term rebound in rainwater pH which has been recorded across many of these areas and which is the result of reductions in the emission of sulfur and nitrogen oxides (De Wit et al., 2007; Monteith et al., 2007; Clark et al., 2010; SanClements et al., 2012).

These widely-observed increases in DOM in surface waters are also supported by data from laboratory experiments substantiating the positive relationship between DOM solubility and the pH of soil (or soil solution), through two processes: (1) increased solubility of Al and Fe ions which strongly complex with DOM (Bohan et al., 1997; Lofts et al., 2001; Qiu et al., 2015); and (2) the addition of acidity which can reduce the solubility of organic matter by increases in intermolecular and intramolecular bonding (Tipping and Woof, 1991; Lumsdon et al., 2005).

In conjunction with large changes in DOM concentration induced by acidification, changes in DOM quality are expected. Hydrophobic DOM requires a greater net charge to become soluble, relative to hydrophilic DOM (Thurman, 1985; Senesi et al., 1991; Tipping and Woof, 1991; Ekström et al., 2011). Decreasing pH therefore lowers the solubility of phenol-rich hydrophobic acids, leading to soil-water dominated by hydrophilic compounds (David et al., 1989; Ekström et al., 2011). The current debate around the effects of acidification on DOM implicitly

assumes that pH increases have the opposite effect.

The effect of acid rain on DOM in different terrains remains controversial due to the heterogeneities in pedology and hydrology (Kennedy et al., 1996; Bohan et al., 1997; Evans et al., 2012; Qiu et al., 2015), and the intervention of climate factors (e.g. air temperature, precipitation) (Evans et al., 2005; Clark et al., 2010; Ritson et al., 2014). For example, many temperate soils rich in clay minerals and organic matter have substantial acid-neutralising capacities (Likens et al., 1996; Schlesinger and Bernhardt, 2013) which show relatively little pH change when they exposed to acid rain. Whereas, strongly acid soils from the humid tropics have little capacity to buffer additional acidity and therefore may respond more quickly to acid deposition. In karstic systems, overlying soils generally contain broken-up carbonate bedrock (Fairchild and Baker, 2012) and should have considerable capacity to buffer the acidity of the soil solution.

Previous cave studies of DOM have mainly focused on the relationship between the variation of DOM and climate changes. On seasonal timescales, DOM concentration in karst dripwaters have been thought to be driven by the flushing of soil DOM which is dependent on production of mobile soil DOM and rainfall exceeding field capacity (e.g. Toth, 1998; Baker and Genty, 1999; van Beynen et al., 2000, 2002; Ban et al., 2008; Tissier et al., 2013). On inter-annual timescales, Cruz et al. (2005) identified that increased DOM concentration and fluorescence intensity in cave dripwaters could be related to increased air temperature in the prior winter, which potentially promoted greater humification in the soil zone and an increased supply of DOM in the following wet season. Furthermore, Ban et al. (2008) have shown that the structure of the DOM peak in dripwaters from Shihua Cave, northern China, varies from year to year, influenced by the intensity and frequency of rainfall. However, the effect of acid rain as a driver of DOM dynamics in karst systems remains largely untested.

When soil DOM is mobilized into the karst aquifer, the transport process in the unsaturated zone (consisting of soil, epikarst and transmission zone (Ford and Williams, 2007; Pronk et al., 2009) also exerts an influence on the concentration of DOM. Many studies of DOM discharge from karst springs have shown higher DOM concentration in the wet season and lower concentration in the dry season, the lower dry season concentration potentially being caused by increased mineralization and degradation of DOM during transit (Emblanch et al., 1998; Batiot et al., 2003; Mudarra and Andreo, 2011; Mudarra et al., 2014). DOM was therefore often considered a useful tracer relative to certain traditional geochemical tracers to characterize the hydrological process (infiltration, residence time) (Emblanch et al., 1998; Batiot et al., 2003). Most of the previous studies on this topic focused on the soil-epikarst where infiltrating water was sensitive to the infiltration event (e.g. Pronk et al., 2009; Mudarra and Andreo, 2011; Tissier et al., 2013; Mudarra et al., 2014). However, studies focusing on the transfer of DOM in the unsaturated zone (transmission zone) are clearly needed to better understand DOM dynamics within the entire karst system.

Southern China following Europe and North America became the third region to suffer from acid rain in the beginning of the 1990s (Fig. 1a) (Larssen et al., 1999; Tang et al., 2010). At the same time, the middle and lower reaches of the Yangtze River have exhibited frequent episodes of droughts and floods over the past ten years. This sensitive region, which is now exposed to climate change and acid rain, offers an opportunity to evaluate the effect of acid rain as well as climate change on the variation of DOM in karst groundwater.

Heshang Cave (30° 27'N, 110° 25'E; 294 m altitude) (Fig. 1a) is situated in the middle reaches of the Yangtze River, southern China (Hu et al., 2008). Previous studies have confirmed that perennial dripwaters in Heshang Cave are fed by the large overlying aquifer reservoir (Duan et al., 2016; Owen et al., 2016), Heshang Cave is

therefore eligible as a sentinel of changes in local karst groundwater quality. In this study, samples of groundwater collected from two drip sites in Heshang Cave between 2005 and 2014 were analyzed using fluorescence spectroscopy to characterize both the quantity and quality of DOM (Baker et al., 2007; Fellman et al., 2010; Bridgeman et al., 2011; Stedmon et al., 2011; Ritson et al., 2014). The long-term DOM record from Heshang Cave also can offer an opportunity to investigate the DOM transfer process and evaluate the residence time of DOM in the unsaturated zone of the karst aquifer.

2. Method

2.1 Study site

The East Asian Monsoon dominates the climate of the study region, with a warm and moist summer, but a relatively cold and dry winter (Fig. 1a). Annual rainfall recorded at Yichang about 90 km away from the study site is 1162 ± 234 mm (1s, $n = 59$, from 1950 to 2008) (Fig. 1b). Approximately 70% of the annual rainfall occurs between May and September, and the annual mean evapotranspiration of the Yichang region from 1985 to 2005 was 734 mm (Zhang and Li, 2006).

Heshang Cave extends sub-horizontally from its mouth on the bank of the Qingjiang River for a distance of ~ 250 m. The cave is developed on the hinge zone of a large N-S anticline within Cambrian dolomite (Fig. 1c) (Hu et al., 2008). The dolomite host rock is permeable due to fracturing and karstification, and thus forms a carbonate aquifer.

The cave is currently located in the unsaturated zone of the aquifer and the entrance of the cave is about 30m above the present day level of the Qingjiang River (Fig. 1c). The thickness of the unsaturated zone above the cave is highly variable from about 50 to 300 m due to a steep terrain (Hu et al., 2008). The dolomite rock is covered by

a discontinuous and thin (~ 30 cm) soil layer derived from wind-blown carbonate bedrock and silicate dust. Human activity was rare due to the precipitous path leading to the cave.

Rainwater infiltrates through fissures and fractures within the unsaturated zone to drip through the cave roof. The cave is wet throughout the year, with active drips, standing pools of water and some flowing water close to the back of the cave during flood events (Hu et al., 2008; Long et al., 2015). Drip sites HS4, HS6 are located ~ 150 m further into the cave, and the distance between the two sites is about 4 m (Fig. 1c). Two coeval columnar stalagmites fed by two drip points (Hu et al., 2008), suggests that more than one steady reservoir exists above cave roof to recharge the two drip sites. The drip rates of two sites can be considered to be fed by fissure flow, according to the classification of Smart and Friedrich (1987). The lack of a geochemical response at two drippoints to the transition from drought to wet conditions (e.g. $\delta^{44/42}\text{Ca}$, $\delta^{18}\text{O}$) suggests that the perennial dripwaters are well mixed, and hence geochemical signals become attenuated between event water and water stored in overlying aquifer reservoirs, consistent with > 1 year of residence time (Duan et al., 2016; Owen et al., 2016).

2.2 Data and water sample collection

Precipitation and air temperature outside the cave since 2003 were measured automatically every 2 hours using a HOBO Data Logging Rain Gauge (RG3-M) and HOBO Pro v2 logger (U23-001), both installed at a ~1.5-meter-high wood shelf on a flat roof of a dwelling in the local village which is ~2 km away from Heshang Cave at a similar elevation. The logger records are identical to those of the meteorological station at Changyang (30°28'N, 111°11'E, 144.2 m) (Fig. 1b) on both seasonal and shorter timescales (Hu et al., 2008).

The dataset of daily rainwater pH was collected from four acid rain monitoring stations including Yichang, Zigui,

Jianshi, and Wufeng around the study site (Fig. 1b). The basic coordinates and distances to Heshang Cave are summarized in Table S1. The span of the dataset was from 2005 to 2015. Data quality was examined by the conductivity of precipitation (K) – pH inequality method proposed by Tang et al. (2008). Analysis of pH values greater than 9.0 or less than 2.0 was not considered reliable and was discarded. The monthly and annual (January to December) pH of rainwater was calculated by volume weighted mean method of concentration of H^+ and rainfall amount.

Water samples from two drip sites were collected at 30~40 day intervals between 2005 and 2014. The samples were collected in 50 ml sealed glass bottles and refrigerated immediately upon return from the field (Li et al., 2014). Drip rates were recorded by manual counting for two minute timespans during each sampling trip and then converted to ml/min by assuming a constant volume of 0.15 ml per drip (Baker and Barnes, 1998). The annual mean drip rate is calculated as the arithmetic mean (unless otherwise stated, also the other parameters discussed herein).

Monthly cumulative rainwater samples were collected in a 5 L HDPE bottle with a funnel which is placed at the wood shelf on the flat roof between 2011 and 2015. The external body of HDPE bottle was covered with foil paper and the bottom of the HDPE bottle was coated with ~ 0.5 cm-thick mineral oil to prevent evaporation. Prior to use for next month, the bottle was cleaned and dried. The sub-samples of the homogenized precipitation were collected into pre-cleaned 8 ml glass sealed bottles for measurement of sulfate concentration.

2.3 Sample analysis

Analysis of DOM was completed on 0.22 μ m filtered dripwater samples using a LS-55 Perkin-Elmer luminescence

spectrophotometer at China University of Geosciences (Wuhan, China). Fluorescence emission spectra at an optimal excitation wavelength of 320 nm were recorded across wavelengths scanning from 200 to 500 nm at 5 nm steps, with slits set to 5 nm for excitation and 20 nm for emission. Analyses were performed at room temperature, and blank water (deionized water) scans were run every 10-15 analyses. The fluorescence intensity for each sample was corrected against the intensity of blank water to eliminate the Rayleigh and Tyndall scatter and partly the Raman scatter (Fig. 2). The reproducibility of the emission spectrum of blank water was relatively high for which the emission intensity at 360 nm averaged out at 210 ± 10 (1s, $n = 12$) arbitrary units (a.u.) during the measurement.

Sulfate concentration in rainwater was analysed using a Dionex ICS-900 system equipped with Chromeleon 7.0 software at Changsha Uranium Geology Research Institute. The ion chromatograph was calibrated using an external standard sulfate solution (GSB 07-1268-2000) to ensure accuracy and stability, with a detection limit of 0.1 mg/L.

Sulfur emissions can be directly linked to the higher acidity of rainfall in this region. Therefore, the pH of rainwater could be calculated by the sulfate concentration in rainwater. Due to a natural background S value exists in rainwater, we assume that the minimum sulfate concentration in rainwater was as the natural background S value, which exists in all local rainwaters; and the pH of natural rainwater with minimum sulfate concentration is defined as 5.6. In addition, we also need to assume that sulfuric acid could ionize completely, that is one mole of S concentration can contribute 2 moles of H^+ . Thus, the equation was as follows:

$$pH_R = -\log_{10}(2 \times \frac{C_R - C_{min}}{M} + 10^{-5.6}) \quad (1)$$

Where C_R is the sulfate concentration in rainwater; C_{min} is the minimum sulfate concentration in rainwater from 2011 to 2015; M is mass number of sulfate; pH_R is the predicted pH of rainwater.

3. Results

3.1 Climate variation

The daily precipitation amount between January 2004 and February 2014 ranged from 0 to 98 mm and the seasonal rhythm of precipitation was characterized by higher rainfall in summer (June-August) and lower rainfall in winter (December-February) (Fig. 3a and cyan bars). As the East Asian monsoon varies in strength from year to year, the annual precipitation amount varied distinctly and ranged from 763 mm to 1354 mm, averaging 984 mm during the monitoring period (Table 1). Mean monthly air temperature between January 2004 and February 2014 ranged from 2.9 to 29.6 °C with the lowest air temperatures recorded in January/February and the highest in July/August (Fig. 3i). Annual mean air temperature varied from 16.4 to 18.4 °C with an average of 17.4 °C (Table 1).

The pH dataset of daily rainwater from four acid rain monitoring stations around Heshang Cave all presented increasing trends during 2005 to 2015 (Fig. S1). The monthly volume-weighted pH series from four stations each exhibited statistically significant increasing trends (Table S1). The monthly pH value from four stations ranged from 3.49 to 6.17 with higher pH values in summer and lower pH values in winter generally, reflecting the relative intensity of the sulfate emission locally with lower rainwater sulfate concentration in summer and higher sulfate concentration in winter (Fig. 4). The annual volume-weighted pH value of rainwater from all stations ranged from 4.18 to 5.22, and showed increasing trends across the study period (Table S1 and Fig. S1).

The sulfate concentration in monthly cumulative rainwater varied across a wide range, from 1.89 to 30.1 mg/L during the period 2011 to 2015, with a higher content in winter and lower content in summer (Fig. 4). According to the equation (1), the predicted pH of local rainwater ranged from 3.53 to 5.60, with higher values in summer and lower values in winter (Fig. 4). The annual volume-weighted predicted pH value ranged from 4.17 to 4.57 with a statistically significant increasing trend (Fig. 5). In spite of the bias between predicted pH value of rainwater in the study site and monitoring pH values of rainwater in Yichang station, the temporal variation of predicted pH in local rainwater is concordant with the temporal pH distribution of Yichang station, which suggested that deposition of acids of two places were synchronous (Fig. 5). As for the bias, it may be related to the incomplete ionization of sulfuric acid. Considering that the pH of rainwater in the study site was mainly responsive to the pH record of Yichang station, the pH dataset of Yichang acid rain station is therefore adopted in the following discussion.

3.2 Dripwater discharge rates

Drip rates ranged from 1.28 to 5.25 ml/min with a mean value of 2.51 ml/min at drip site HS4, and 0.75 to 2.25 ml/min at site HS6, with a mean value of 1.28 ml/min (Fig. 3b and 3e; Table 1). The seasonal variation in drip rates was more sensitive to seasonal rainfall than daily rain events with higher drip rates in summer and slower drip rates in winter generally (~ 2 ml/min for HS4, ~ 1 ml/min for HS6) (Fig. 3b and 3e, blue horizontal dash lines). Compared with the drip rate of HS6, HS4 had a shorter lag time and was more sensitive in its response to seasonal rainfall variations (Fig. 3b and 3e), this difference arising due to differences in the hydrologic network feeding these drips. On annual timescales, the annual mean value of each drip rate varied from 1.83 to 3.40 ml/min for HS4 and from 0.95 to 1.72 ml/min for HS6. Both were consistent with annual precipitation with faster drip rates in wetter years and slower drip rates in dryer years (Table 1).

3.3 Fluorescence

The emission spectra at an excitation wavelength 320 nm shows three distinct peaks (Fig. 2a). After subtracting the intensity of blank water, only a single peak remained with a fluorescence wavelength maxima varying between 399 nm and 410.5 nm, and with a mean value of 405.3 nm for HS4, and varying between 397.5 nm and 414.5 nm with a mean value was 405.1 nm for HS6 (Fig. 3c and 3f). The fluorophore within this spectral range corresponds to humic-like materials that have been identified in surface water (Baker et al., 2008) and karst cave water (Hartland et al., 2010), supporting the use of fluorescence as an analogue for DOM in this study. The fluorescence wavelength maxima time series of two dripwaters had no perceptible intra-annual or inter-annual variations (Fig. 3c and 3f), which would be expected if significant compositional changes in DOM had occurred over the study period (Tipping and Woof, 1991).

The fluorescence intensity of HS4 varied between 151.7 and 428.4 a.u. with a mean value of 229.6 a.u. (Fig. 3d and Table 1), and the fluorescence intensity for HS6 varied between 155.0 and 733.3 a.u. with a mean value of 253.9 a.u. (Fig. 3g and Table 1). Fluorescence intensity time series of the two dripwaters showed similar variations. On seasonal timescales, fluorescence intensity generally showed higher values in summer (Fig. 3, cyan bars) and lower values in winter (~180 a.u. of HS4, ~210 a.u. for HS6) (Fig. 3d and 3g, blue horizontal dash lines), although several significant peaks occurred in dry seasons (outside of the cyan bars). On inter-annual timescales, the annual mean fluorescence intensity varied between 174.2 and 313.8 a.u. for HS4 and between 217.7 and 316.8 a.u. for HS6 (Table 1). Compared with the fluorescence intensity of HS6, HS4 had longer and frequent high values rather than transient single peaks (Fig. 3d and 3g); moreover, the occurrence of high fluorescence values in HS4 dripwater seem to have generally occurred earlier than in HS6 dripwater. To a first approximation, the mean annual

fluorescence intensity value of each dripwater appears to respond to the annual rainfall amount (with a one year lag). For example, the low annual fluorescence intensity in 2007 corresponded to the low annual rainfall in 2006, and high annual fluorescence intensity in 2009 corresponded to the high annual rainfall in 2008 (Table 1).

4. Discussion

4.1 Hydraulic response and DOM transport

Delayed hydraulic responses and DOM transport times after aquifer recharge events have been observed in karstic systems before, and are generally attributed to the effect of the soil moisture deficit and the hydrologic decoupling of soil-aquifer systems, in delaying water and solute transport (e.g. Emblanch et al., 1998; Genty and Deflandre, 1998; Batiot et al., 2003; Pronk et al., 2009; Charlier et al., 2010, 2012; Tissier et al., 2013). Continuous monitoring provides the opportunity to quantify this lag time between rainfall, drip discharge, and DOM breakthrough (Tissier et al., 2013; Riechelmann et al., 2016). Cross-correlations with a 3-point running average over the monitoring period were computed. The cross-correlation between rainfall (calculated as average daily precipitation) and fluorescence intensity showed an optimal correlation coefficient ($r_{HS4} = 0.51$, $r_{HS6} = 0.40$, $p < 0.01$) with some ~11 months of lag for HS4, and ~13 months for HS6, and the rainfall/drip rate cross-correlation showed an optimal correlation coefficient ($r_{HS4} = 0.80$, $r_{HS6} = 0.58$, $p < 0.01$) with 0 months lag for HS4 and ~3 months lag for HS6 (Fig. 6). It is noteworthy that the rainfall/fluorescence intensity cross-correlation for HS6 also exhibits a significant correlation coefficient ($r_{HS6} = 0.39$, $p < 0.01$) with 0 months lag (Fig. 6). Considering that drip rate is more sensitive to rainfall than DOM fluorescence, we assert that the lag time of ~13 months is more credible than 0 months for the fluorescence intensity of HS6. The disparate lag time for drip rate and fluorescence intensity can be reconciled by the different mechanisms driving the response of DOM and drip rate to rainfall.

Compared with fluorescence intensity variation, the sensitive response of drip rates to rainfall can be explained by the change of head pressure affecting dripwaters: in summer, higher rainfall will increase the head pressure and then promote faster drip rates, in winter, low rainfall had a limited effect on head pressure, so drip rates remained fairly constant, being recharged by base flow from the overlying reservoir (Fig. 3b and 3e). In this case, the seasonal lag in summer is expected to produce a negligible bias on inter-annual timescales. Thus, we could calculate the relationship between annual precipitation amount and annual mean drip rate without any lag (Fig. 7):

$$[DR]_{HS4} = 0.0025 [APA] + 0.16 (R^2 = 0.80, n = 9, p < 0.01) \quad (2)$$

$$[DR]_{HS6} = 0.0010 [APA] + 0.32 (R^2 = 0.86, n = 9, p < 0.01) \quad (3)$$

In equations (2) and (3), [DR] and [APA] are initialisms of drip rate and annual precipitation amount, respectively. The slopes reflect the sensitivity of the two drip sites to local annual precipitation amount. However, we cannot interpret the significance of the intercepts which should correspond to the constant value of base flow recharged by the overlying reservoir (Fig. 3b and 3e, blue horizontal dash lines). Some case studies had deduced that drip rates in karstic caves respond to water excess rather than rainfall amount (Genty and Deflandre, 1998; Riechelmann et al., 2016). Considering the annual mean evapotranspiration of Yichang region was 734 mm from 1985 to 2005 (Zhang and Li, 2006). Thus, we also introduced the constant (734) and transfer the equations (2) and (3) as follow:

$$[DR]_{HS4} = 0.0025([APA] - 734) + 2.00 (R^2 = 0.80, n = 9, p < 0.01) \quad (4)$$

$$[DR]_{HS6} = 0.0010([APA] - 734) + 1.06 (R^2 = 0.86, n = 9, p < 0.01) \quad (5)$$

In equations (4) and (5), the values between parentheses give the local annual effective rainfall amount. As expected, the values of the intercepts in these equations were close to the constant value of the base flow of two

dripwaters respectively. The results suggest that the drip rates were dominated by local effective rainfall amount which could modulate head pressure overlying the two drip sites on inter-annual timescales.

In terms of fluorescence intensity, the ~1 year lag can be comprehended as the product of two sets of processes: (1) soil humification process (Lofts et al., 2001; Michalzik et al., 2003; Blyth et al., 2008) and (2) aquifer processes (Emblanch et al., 1998; Batiot et al., 2003; Pronk et al., 2009; Charlier et al., 2010, 2012; Tissier et al., 2013).

Previous studies have suggested that the decomposition rate of soil organic matter (SOM) varies considerably, and that SOM can be divided into different pools with contrasting decay times which can be broadly seen to range between an old fraction that decays slowly ($\sim 10^2$ - 10^3 year), and a young fraction that decays very quickly (~ 1 year). The ^{14}C evidence from HS4 stalagmite fed by HS4 dripwater showed that the organic matter in HS4 is long-lived (Noronha et al., 2015), so we can disregard the possible role of young organic matter. Furthermore, the geochemical evidence from the HS4 drip site, especially the invariant calcium isotope ratio ($\delta^{44/42}\text{Ca}$) value, points to a long (> 1 year) groundwater residence time (Owen et al., 2016). Weighing the contribution of the two processes, the lag is most sensibly ascribed to an efficient transport process from soil to drip point (the effect of the soil moisture deficit and the karst process on delaying water and solute transport) instead of a rapid soil humification process.

Considering of the effect of sampling frequency, a 3-point running-average was used in the evaluation of lag time of fluorescence intensity, the average lag time of the two drip sites (1 year) was used to define the lag time between the climate signal and the fluorescence intensity of dripwaters (Fig. 8). Notably, several significant peaks remained outside the cyan bars after eliminating a one year lag. We inferred that these peaks were related to the seasonal rainfall distribution which varies somewhat from year to year.

On inter-annual timescales, the robust linear relationship between annual precipitation amount and annual mean fluorescence intensity with a one year lag, is statistically stronger than the relationship without any lag (Fig. 9):

$$[FI]_{HS4} = 0.207([APA] - 734) + 177.5 \quad (R^2 = 0.86, n = 9, p < 0.01) \quad (6)$$

$$[FI]_{HS6} = 0.176([APA] - 734) + 209.5 \quad (R^2 = 0.77, n = 9, p < 0.01) \quad (7)$$

Where [FI] is the initialisms of fluorescence intensity. Similar to equations (4) and (5), only considering [APA] and annual mean evapotranspiration as a whole, the significance of intercepts in equation (6) and (7) can be interpreted as the DOM concentration of base flow from the overlying reservoir. Equation (6) and (7) suggested that the annual mean fluorescence intensity was actually governed by local effective annual rainfall amount on inter-annual timescales.

Although only separated by some ~4 meters in the cave, the two drip points diverged significantly in their hydrologic characteristics. Compared with HS4, the drip rate of HS6 was slower and more hysteretic to rainfall. We inferred that one larger reservoir recharged the HS6 drip site, one with a higher capability to buffer the infiltrating water. Thus, the lower sensitivity of HS6 to rainfall (smaller slope) was readily understood. In this case, longer residence times would cause the peak of HS6 drip rate and fluorescence intensity to occur later than for HS4.

4.2 Rainfall

Rainfall, air temperature and pH of rainwater are three important factors capable of affecting the seasonal input of soil DOM to the karst aquifer, and the subsequent DOM concentration in dripwater in our study site. The seasonal variations of DOM with high values in summer and constant low values in winter is consistent with the seasonal

nature of rainfall, air temperature and rainfall pH. However, the congruent seasonal pacing and amplitude between fluorescence intensity and precipitation (Fig. 8), as opposed to the sharp seasonal rhythms of air temperature (Fig. 3i), and increasing seasonal pH value of rainfall (Fig. 5), suggests that summer rainfall is the more prominent factor controlling the flushing of SOM in the Asian monsoon region (Ban et al., 2008).

In the winter, the low pH of rainwater, low air temperature and precipitation amounts are conducive to the retention and preservation of organic matter in karst (Kalbitz et al., 2000; Evans et al., 2005; Conant et al., 2011; Ekström et al., 2011). The fluorescence intensity of dripwaters during the winter season therefore mainly reflects the characteristics of the base flow component from the overlying reservoir (Fig. 3d and 3g, blue horizontal dash lines); when the coming spring approaches, SOM decomposition and depolymerization are likely enhanced as temperatures rise (Kalbitz et al., 2000; Conant et al., 2011), and with the approach of the monsoon (in May generally), soil DOM is mobilized and transported by strong rainfall (Ban et al., 2008). When soil leachate enters the unsaturated zone of the karst aquifer, mineralization and degradation of DOM during the transfer process affects the DOM concentration. Compared with baseflow in winter generally, the infiltrating water in summer has a shorter time to mineralize and degrade, and promote higher DOM in dripwaters in summer (Thurman, 1985; Emblanch et al., 1998; Batiot et al., 2003; Mudarra and Andreo, 2011; Mudarra et al., 2014).

The annual (effective) precipitation amount can affect the concentration of DOM in dripwaters through three different processes on inter-annual timescales: (1) more humid soil environments are favorable to the humification rate of SOM in the study site (Christ and David, 1996; Tipping et al., 1999; McGarry and Baker, 2000), which acts to increase the production of transportable DOM in the soil; (2) the greater annual precipitation amount tends to occur with more strong rainfall events, contributing to the flushing and transportation of soil DOM (Toth, 1998;

Baker and Genty 1999; van Beynen et al., 2000, 2002; Tissier et al., 2013). (3) the greater annual precipitation amount will increase the head pressure and decrease the residence time of infiltrating water, lessening the influence of mineralization and degradation on DOM, which will thereby promote higher annual DOM concentration in summer discharges (Thurman, 1985; Emblanch et al., 1998; Batiot et al., 2003; Mudarra and Andreo, 2011; Mudarra et al., 2014). These three processes likely act in unison to magnify the precipitation signal imprinted in the fluorescence intensity of dripwater in Heshang Cave.

4.3 Air temperature

Air temperature can control the humification rate and mineralization of organic matter in soil and solution (Oades, 1988; Davidson and Janssens, 2006; Schipper et al., 2014). Cruz et al. (2005) investigated the relationship between the fluorescence intensity of dripwaters from Santana Cave located in southeastern Brazil and local climate in two hydrological years, and found that the annual mean value of fluorescence intensity was sensitive to an increase of 5.5 °C in mean winter temperature in the previous year. However, the fluorescence intensity of dripwaters in Heshang Cave appeared to be insensitive to local air temperature on either intra-annual or inter-annual timescales (Fig. 3 and 10). We calculate the inter-seasonal and inter-annual air temperature variation during 2004 to 2014 which the Heshang Cave region experienced to be much smaller than that observed in Brazil by Cruz et al. (2005). Over the nine years during which monitoring was conducted, air temperatures in summer ranged between 25.3 to 28.4 °C (Δ 3.1 °C), and 5.8 to 8.7 °C (Δ 3.2 °C) during the winter. The annual average air temperatures ranged between 16.4 to 18.4 °C, a variation of 2.0 °C, relative to 5.5 °C observed at Santana Cave. The large variation in rainfall in the locality of Heshang Cave (between 763 mm/yr and 1354 mm/yr from 2005 to 2013), is therefore likely to obscure the intrinsic air temperature sensitivity of substrate decomposition (Schipper et al., 2014), causing

a lower observed 'apparent' air temperature sensitivity as inferred from the fluorescence intensity measurements (Davidson and Janssens, 2006).

4.4 pH of rainfall

A little bias may exist in using rainfall pH of Yichang acid rain station to represent the pH of rainfall in the vicinity of Heshang Cave. In our analysis we focused on the linear pH regression over the eleven-year rainfall dataset from 2005 to 2015 (Fig. 5), which provides as a measure of the average change in rain pH over the study period. Laboratory experiments and field investigations have substantiated that pH varies positively with the quantity and quality of DOM in soil-water (e.g. Evans et al., 2005; Clark et al., 2010; Ekström et al., 2011; Qiu et al., 2015). The monthly and annual volume-weighted pH value of rainwater in this study showed a significant ascending trend ranging from 3.49 to 5.85 and from 4.19 to 5.13 respectively around the cave during 2005 to 2015 (Fig. 5 and 11). If soil DOM showed a response to these pH variations, it is reasonable to expect that the fluorescence intensity time series should also show a similar ascending trend, corresponding to a DOM increase in response to the pH recovery (Monteith et al., 2007). However, the monitoring results showed that fluorescence intensity followed a descending trend on monthly and annual timescales (Fig. 3 and 11), although not statistically significant, consistent with the variation of precipitation amount (Fig. 3 and 11), and contrary to the pH trend (Fig. 5 and 11). This suggests that the aquifer DOM concentration was insensitive to acid rain at Heshang Cave. The quality of DOM can be reflected by the variation of the fluorescence wavelength maxima, which is also susceptible to the variation of pH. Increasing pH can raise the solubility of the hydrophobic acids, leading to a soil-water more dominated by hydrophobic compounds characterized by high aromaticity, molecular weight and longer peak fluorescence wavelength; and vice versa (David et al., 1989; Ekström et al., 2011). However, no trends were

observed in the variation in fluorescence wavelength maxima (Fig. 3c and 3f), suggesting that the quality of DOM was also indifferent to variations in the pH of rainwater. This phenomenon has been viewed in laboratory leaching experiments. Qiu et al. (2015) conducted a laboratory leaching column experiment with an intact acid forest soil column from southern China and found that soil and soil solution chemistry (including DOM, Al and Fe) are not affected by an influent solution with a $\text{pH} \approx 4.5$. Furthermore, Evans et al. (2012) found that further pH increases towards alkaline values generated only a slight additional increases in DOC concentration at the Migneint podzol site with a soil pretreatment pH of 4.4. The similar results from laboratory leaching experiments and our monitoring data indicate that current acid rain ($\sim\text{pH}$ 5.6 to ~ 4.5) will have a limited effect on the dissolution of DOM in karst soil pore waters. Although some reasons for this lack of sensitivity have been proposed (Evans et al., 2012; Qiu et al., 2015), we infer that it was likely to be linked to the buffering capacity of karst soil in the Heshang region consisting of carbonate debris (Noronha et al., 2015; Yun et al., 2016) which can buffer the low pH values of rainwater rapidly on contact with infiltration (Bowman et al., 2008).

5. Conclusions

A monthly resolution, nine-year monitoring study of duplicate fluorescence intensity measurements of two dripwaters in Heshang Cave, Southern China provides insights into the hydrological characteristics and the drivers of DOM mobilization on different timescales and allows us to reach the following conclusions.

1. The cross-correlation analysis is an efficient method to investigate the lag time between different variables of dripwaters and external environmental variables. In Heshang Cave, discharge of drip sites can respond to rainfall quickly with relatively short lag times due to the modulation of head pressure on intra-annual and inter-annual timescales. Compared with drip rates, the fluorescence intensity in dripwaters displayed longer lag times (~ 1 year)

from soil to drip sites, reflecting the physical transport of DOM through the aquifer system. In addition, compared with some traditional geochemical tracers, DOM can be an efficient tracer to investigate the transfer pathway of DOM and evaluate the ability to trace residence time in the unsaturated zone of the karst aquifer.

2. After eliminating the one year lag in our data, the congruent seasonal pacing and amplitude between fluorescence intensity and rainfall suggested that in Heshang Cave, seasonal DOM variations were mainly a response to seasonal precipitation distribution which can determine the output of DOM from the soil layer, and the mineralization and degradation of DOM during transport. This result is comparable to monitoring results in other regions. On inter-annual timescales, a robust linear relationship between fluorescence intensity and annual (effective) precipitation amount implies that precipitation is the most important determinant for DOM concentration in karst aquifers through three processes: (1) humification rate of SOM; (2) flushing and transport following strong rainfall; (3) mineralization and degradation of DOM within transfer processes.

3. Combined with previous results from laboratory leaching experiments, the insensitivity of fluorescence intensity and fluorescence wavelength maxima of unsaturated zone flow to the local pH of acid rain on intra-annual and inter-annual time scales implies that current acid rain ((~pH 5.6 to ~4.5) has a limited effect on the dissolution of DOM in karst soil and soil solution.

4. The results presented permit an improved understanding of the influence of climate and acid rain on DOM mobilization into karst aquifers on intra/inter-annual scales. However, Heshang Cave is only a case study, it would be necessary in future studies to assess whether and how geographic differences between karstic systems influences on the contribution of climate and acid rain to DOM mobilization into karst aquifers.

Acknowledgements

The authors thank Zhifang Xiong, Zhenhua Cao, Luyao He, Zhongwu Ma, Erpu Shen, Jiaqi Zhou, Zhenhui Yi, Feifei Chen, Niu Li, Kaihui Xia, Yuezhong Shi, Yuhui Liu, Mingda Wang, Qin Li, Yu Shi, Chengzhan Li, Qixi Mao, Liangliang Bao and Shouwu Qin for assistance with field sampling. This work was funded by the National Natural Science Foundation of China (Grants No. 41371216, 41072262 and 41130207).

References

- Andrade-Eiroa, Á., Canle, M., Cerdá, V., 2013. Environmental applications of excitation-emission spectrofluorimetry: an in-depth review II. *Applied Spectroscopy Reviews*, 48, 77-141.
- Baker, A., Barnes, W.L., 1998. Comparison of the luminescence properties of waters depositing flowstone and stalagmites at Lower Cave, Bristol. *Hydrological Processes*, 12, 1447-1459.
- Baker, A., Genty, D., 1999. Fluorescence wavelength and intensity variations of cave waters. *Journal of Hydrology*, 217, 19-34.
- Baker, A., Elliott, S., Lead, J.R., 2007. Effects of filtration and pH perturbation on freshwater organic matter fluorescence. *Chemosphere*, 67, 2035-2043.
- Baker, A., Tipping, E., Thacker, S.A., Gondar, D., 2008. Relating dissolved organic matter fluorescence and functional properties. *Chemosphere*, 73, 1765-1772.
- Ban, F., Pan, G., Zhu, J., Cai, B., Tan, M., 2008. Temporal and spatial variations in the discharge and dissolved organic carbon of drip waters in Beijing Shihua Cave, China. *Hydrological Processes*, 22, 3749-3758.
- Batiot, C., Liñán, C., Andreo, B., Emblanch, C., Carrasco, F., Blavoux, B., 2003. Use of Total Organic Carbon (TOC) as tracer of diffuse infiltration in a dolomitic karstic system: The Nerja Cave (Andalusia, southern Spain). *Geophysical research letters*, 30, 2179.
- Blyth, A.J., Baker, A., Collins, M.J., Penkman, K.E.H., Gilmour, M.A., Moss, J.S., Genty, D., Drysdale, R., 2008. Molecular organic matter in speleothems and its potential as an environmental proxy. *Quaternary Science Reviews*, 27, 905-921.

Bohan, L., Seip, H.M., Larssen, T., 1997. Response of two Chinese forest soils to acidic inputs: leaching experiment. *Geoderma*, 75, 53-73.

Bowman, W.D., Cleveland, C.C., Halada, Ľ., Hreško, J., Baron, J.S., 2008. Negative impact of nitrogen deposition on soil buffering capacity. *Nature Geoscience*, 1, 767-770.

Bridgeman, J., Bieroza, M., Baker, A., 2011. The application of fluorescence spectroscopy to organic matter characterisation in drinking water treatment. *Reviews in Environmental Science and Bio/Technology*, 10, 277-290.

Charlier, J.B., Bertrand, C., Binet, S., Mudry, J., Bouillier, N., 2010. Use of continuous measurements of dissolved organic matter fluorescence in groundwater to characterize fast infiltration through an unstable fractured hillslope (Valabres rockfall, French Alps). *Hydrogeology Journal*, 18, 1963-1969.

Charlier, J.B., Bertrand, C., Mudry, J., 2012. Conceptual hydrogeological model of flow and transport of dissolved organic carbon in a small Jura karst system. *Journal of Hydrology*, 460-461, 52-64.

Christ, M.J., David, M.B., 1996. Temperature and moisture effects on the production of dissolved organic carbon in a Spodosol. *Soil Biology and Biochemistry*, 28, 1191-1199.

Clark, J.M., Bottrell, S.H., Evans, C.D., Monteith, D.T., Bartlett, R., Rose, R., Newton, R.J., Chapman, P.J., 2010. The importance of the relationship between scale and process in understanding long-term DOC dynamics. *Science of The Total Environment*, 408, 2768-2775.

Conant, R.T., Ryan, M.G., Ågren, G.I., Birge, H.E., Davidson, E.A., Eliasson, P.E., Evans, S.E., Frey, S.D.,

Giardina, C.P., Hopkins, F.M., Hyvönen, R., Kirschbaum, M.U.F., Lavalley, J.M., Leifeld, J., Parton, W.J.,

Steinweg, J.M., Wallenstein, M.D., Wetterstedt, M.J.Å., Bradford, M.A., 2011. Temperature and soil organic

matter decomposition rates – synthesis of current knowledge and a way forward. *Global Change Biology*, 17, 3392-3404.

Cruz Jr, F.W., Karmann, I., Magdaleno, G.B., Coichev, N., Viana Jr, O., 2005. Influence of hydrological and climatic parameters on spatial-temporal variability of fluorescence intensity and DOC of karst percolation waters in the Santana Cave System, Southeastern Brazil. *Journal of Hydrology*, 302, 1-12.

David, M.B., Vance, G.F., Rissing, J.M., Stevenson, F.J., 1989. Organic carbon fractions in extracts of O and B horizons from a New England spodosol: effects of acid treatment. *Journal of Environmental Quality*, 18, 212-217.

Davidson, E.A., Janssens, I.A., 2006. Temperature sensitivity of soil carbon decomposition and feedbacks to climate change. *Nature*, 440, 165-173.

De Wit, H.A., Mulder, J., Hindar, A., Hole, L., 2007. Long-term increase in dissolved organic carbon in streamwaters in Norway is response to reduced acid deposition. *Environmental Science & Technology*, 41, 7706-7713.

Duan, W., Ruan, J.Y., Luo, W.J., Li, T.Y., Tian, L.J., Zeng, G.N., Zhang, D.Z., Bai, Y.J., Li, J.L., Tao, T., Zhang, P.Z., Baker, A., Tan, M., 2016. The transfer of seasonal isotopic variability between precipitation and drip water at eight caves in the monsoon regions of China. *Geochimica et Cosmochimica Acta*, 183, 250-266.

Ekström, S.M., Kritzberg, E.S., Kleja, D.B., Larsson, N., Nilsson, P.A., Graneli, W., Bergkvist, B., 2011. Effect of acid deposition on quantity and quality of dissolved organic matter in soil–water. *Environmental Science & Technology*, 45, 4733-4739.

Emblanch, C., Blavoux, B., Puig, J.M., Mudry, J., 1998. Dissolved organic carbon of infiltration within the

autogenic karst hydrosystem. *Geophysical research letters*, 25, 1459-1462.

Evans, C.D., Monteith, D.T., Cooper, D.M., 2005. Long-term increases in surface water dissolved organic carbon: Observations, possible causes and environmental impacts. *Environmental Pollution*, 137, 55-71.

Evans, C.D., Jones, T.G., Burden, A., Ostle, N., Zieliński, P., Cooper, M.D.A., Peacock, M., Clark, J.M., Oulehle, F., Cooper, D., Freeman, C., 2012. Acidity controls on dissolved organic carbon mobility in organic soils. *Global Change Biology*, 18, 3317-3331.

Fairchild, I.J., Baker, A., 2012. *Speleothem science: From process to past environments*. Wiley-Blackwell, Chichester, England.

Fellman, J.B., Hood, E., Spencer, R.G., 2010. Fluorescence spectroscopy opens new windows into dissolved organic matter dynamics in freshwater ecosystems: A review. *Limnology and Oceanography*, 55, 2452-2462.

Ford, D.C., Williams, P.W., 2007. *Karst hydrogeology and geomorphology*. John Wiley & Sons Ltd, England.

Genty, D., Deflandre, G., 1998. Drip flow variations under a stalactite of the Pere Noel cave (Belgium). Evidence of seasonal variations and air pressure constraints. *Journal of Hydrology*, 211, 208-232.

Graham, P.W., Baker, A., Andersen, M.S., Acworth, I., 2015. Field Measurement of Fluorescent Dissolved Organic Material as a Means of Early Detection of Leachate Plumes. *Water, Air, & Soil Pollution*, 226, 1-18.

Hartland, A., Fairchild, I.J., Lead, J.R., Zhang, H., Baalousha, M. 2011. Size, speciation and lability of NOM-metal complexes in hyperalkaline cave dripwater. *Geochimica et Cosmochimica Acta*, 75, 7533-7551.

Hartland, A., Fairchild, I.J., Lead, J.R., Baker, A., 2010. Fluorescent properties of organic carbon in cave

dripwaters: Effects of filtration, temperature and pH. *Science of The Total Environment*, 408, 5940-5950.

Hartland, A., Fairchild, I.J., Lead, J.R., Borsato, A., Baker, A., Frisia, S., Baalousha, M., 2012. From soil to cave:

Transport of trace metals by natural organic matter in karst dripwaters. *Chemical Geology*, 304-305, 68-82.

Hartland, A., Fairchild, I.J., Müller, W., Dominguez-Villar, D., 2014. Preservation of NOM-metal complexes in a modern hyperalkaline stalagmite: Implications for speleothem trace element geochemistry. *Geochimica et Cosmochimica Acta*, 128, 29-43.

Hartland, A., Larsen, J.R., Andersen, M.S., Baalousha, M., O'Carroll, D., 2015. Association of arsenic and phosphorus with iron nanoparticles between streams and aquifers: Implications for arsenic mobility. *Environmental science & technology*, 49, 14101-14109.

Hartmann, A., Kobler, J., Kralik, M., Dimböck, T., Humer, F., Weiler, M., 2016. Model-aided quantification of dissolved carbon and nitrogen release after windthrow disturbance in an Austrian karst system. *Biogeosciences*, 13, 159-174.

Hu, C.Y., Henderson, G.M., Huang, J.H., Chen, Z.H., Johnson, K.R., 2008. Report of a three-year monitoring programme at Heshang Cave, Central China. *International Journal of Speleology*, 37, 143-151.

Jiang, Y., Wu, Y., Groves, C., Yuan, D., Kambesis, P., 2009. Natural and anthropogenic factors affecting the groundwater quality in the Nandong karst underground river system in Yunan, China. *Journal of Contaminant Hydrology*, 109, 49-61.

Kalbitz, K., Solinger, S., Park, J.-H., Michalzik, B., Matzner, E., 2000. Controls on the dynamics of dissolved organic matter in soils: a review. *Soil Science*, 165, 277-304.

- Kennedy, J., Billett, M., Duthie, D., Fraser, A., Harrison, A., 1996. Organic matter retention in an upland humic podzol; the effects of pH and solute type. *European Journal of Soil Science*, 47, 615-625.
- Klučáková, M., Kalina, M., 2015. Diffusivity of Cu (II) ions in humic gels—influence of reactive functional groups of humic acids. *Colloids and Surfaces A: Physicochemical and Engineering Aspects*, 483, 162-170.
- Larssen, T., Seip, H.M., Semb, A., Mulder, J., Muniz, I.P., Vogt, R.D., Lydersen, E., Angell, V., Tang, D.G., Eilertsen, O., 1999. Acid deposition and its effects in China: an overview. *Environmental Science & Policy*, 2, 9-24.
- Lead, J.R., Wilkinson, K.J., 2006. Aquatic colloids and nanoparticles: Current knowledge and future trends. *Environmental Chemistry*, 3, 159-171.
- Li, X., Hu, C., Liao, J., Bao, L., Mao, Q., 2014. An improved method for fluorescence analysis of dissolved organic matter in cave drip water. *Frontiers of Earth Science*, 8, 595-598.
- Likens, G.E., Driscoll, C.T., Buso, D.C., 1996. Longterm effects of acid rain: Response and recovery of a forest ecosystem. *Science*, 272, 244-246.
- Lofts, S., Simon, B.M., Tipping, E., Woof, C., 2001. Modelling the solid-solution partitioning of organic matter in European forest soils. *European Journal of Soil Science*, 52, 215-226.
- Long, X., Sun, Z.Y., Zhou, A.G., Liu, D.L., 2015. Hydrogeochemical and isotopic evidence for flow paths of karst waters collected in the Heshang Cave, Central China. *Journal of Earth Science*, 26, 149-156.
- Lumsdon, D.G., Stutter, M.I., Cooper, R.J., Manson, J.R., 2005. Model Assessment of Biogeochemical Controls on Dissolved Organic Carbon Partitioning in an Acid Organic Soil. *Environmental Science & Technology*, 39,

8057-8063.

McCormack, T., Naughton, O., Johnston, P., Gill, L., 2016. Quantifying the influence of surface water-groundwater interaction on nutrient flux in a lowland karst catchment. *Hydrology and Earth System Sciences*, 20, 2119-2133.

McGarry, S.F., Baker, A., 2000. Organic acid fluorescence: applications to speleothem palaeoenvironmental reconstruction. *Quaternary Science Reviews*, 19, 1087-1101.

Michalzik, B., Tipping, E., Mulder, J., Gallardo Lancho, J.F., Matzner, E., Bryant, C., Clarke, N., Lofts, S., Vicente Esteban, M.A., 2003. Modelling the production and transport of dissolved organic carbon in forest soils. *Biogeochemistry*, 66, 241-264.

Monteith, D.T., Stoddard, J.L., Evans, C.D., de Wit, H.A., Forsius, M., Hogasen, T., Wilander, A., Skjelkvale, B.L., Jeffries, D.S., Vuorenmaa, J., Keller, B., Kopacek, J., Vesely, J., 2007. Dissolved organic carbon trends resulting from changes in atmospheric deposition chemistry. *Nature* 450, 537–540.

Mudarra, M., Andreo, B., 2011. Relative importance of the saturated and the unsaturated zones in the hydrogeological functioning of karst aquifers: The case of Alta Cadena (Southern Spain). *Journal of Hydrology*, 397, 263-280.

Mudarra, M., Andreo, B., Barberá, J.A., Mudry, J., 2014. Hydrochemical dynamics of TOC and NO_3^- contents as natural tracers of infiltration in karst aquifers. *Environmental earth sciences*, 71, 507-523.

Noronha, A.L., Johnson, K.R., Southon, J.R., Hu, C., Ruan, J., McCabe-Glynn, S., 2015. Radiocarbon evidence for decomposition of aged organic matter in the vadose zone as the main source of speleothem carbon. *Quaternary*

Science Reviews, 127, 37-47.

Oades, J., 1988. The retention of organic matter in soils. *Biogeochemistry*, 5(1), 35-70.

Owen, R.A., Day, C.C., Hu, C.Y., Liu, Y.H., Pointing, M.D., Blättler, C.L., Henderson, G.M., 2016. Calcium isotopes in caves as a proxy for aridity: Modern calibration and application to the 8.2 kyr event. *Earth and Planetary Science Letters*, 443, 129-138.

Papageorgiou, A., Papadakis, N., Voutsas, D., 2016. Fate of natural organic matter at a full-scale Drinking Water Treatment Plant in Greece. *Environmental Science and Pollution Research*, 23, 1841-1851.

Pronk, M., Goldscheider, N., Zopfi, J., Zwahlen, F., 2009. Percolation and particle transport in the unsaturated zone of a karst aquifer. *Ground water*, 47, 361-369.

Qiu, Q., Wu, J., Liang, G., Liu, J., Chu, G., Zhou, G., Zhang, D., 2015. Effects of simulated acid rain on soil and soil solution chemistry in a monsoon evergreen broad-leaved forest in southern China. *Environmental Monitoring and Assessment*, 187, 1-13.

Riechelmann, S., Schröder-Ritzrau, A., Spötl, C., Riechelmann, D.F.C., Richter, D.K.R., Mangini, A., Frank, N., 2016. Sensitivity of Bunker Cave to climatic forcings highlighted through multi-annual monitoring of rain-, soil-, and dripwaters. *Chemical Geology*, 449, 194-205.

Ritson, J.P., Graham, N.J.D., Templeton, M.R., Clark, J.M., Gough, R., Freeman, C., 2014. The impact of climate change on the treatability of dissolved organic matter (DOM) in upland water supplies: A UK perspective. *Science of the Total Environment*, 473-474, 714-730.

Rutledge, H., Baker, A., Marjo, C., Andersen, M.S., Graham, P.W., Cuthbert, M.O., Rau, G.C., Roshan, H.,

Markowska, M., Mariethoz, G., Jex, C., 2014. Dripwater organic matter and trace element geochemistry in a semi-arid karst environment: Implications for speleothem paleoclimatology. *Geochimica et Cosmochimica Acta*, 135, 217-230.

SanClements, M.D., Oelsner, G.P., McKnight, D.M., Stoddard, J.L., Nelson, S.J., 2012. New insights into the source of decadal increases of dissolved organic matter in acid-sensitive lakes of the Northeastern United States. *Environmental Science & Technology*, 46, 3212-3219.

Schiperski, F., Zirlewagen, J., Hillebrand, O., Nödler, K., Licha, T., Scheytt, T., 2015. Relationship between organic micropollutants and hydro-sedimentary processes at a karst spring in south-west Germany. *Science of the Total Environment*, 532, 360-367.

Schlesinger, W.H., Bernhardt, E.S., 2013. *Biogeochemistry: an analysis of global change*. Third edition. Elsevier/Academic Press, New York, New York, USA.

Schipper, L.A., Hobbs, J.K., Rutledge, S., Arcus, V.L., 2014. Thermodynamic theory explains the temperature optima of soil microbial processes and high Q10 values at low temperatures. *Global Change Biology*, 20, 3578-3586.

Senesi, N., Miano, T.M., Provenzano, M.R., BRUNETTI, G., 1991. Characterization, differentiation, and classification of humic substances by fluorescence spectroscopy. *Soil Science*, 152, 259-271.

Shen, Y., Chapelle, F.H., Strom, E.W., Benner, R., 2015. Origins and bioavailability of dissolved organic matter in groundwater. *Biogeochemistry*, 122, 61-78.

Smart, P.L., Friedrich, H., 1987. Water movement and storage in the unsaturated zone of a maturely karstified

aquifer, Mendip Hills, England, Proceedings, Conference on Environmental Problems in Karst Terrains and their Solution, Bowling Green, Kentucky. National Water Well Association.

Stedmon, C.A., Seredyńska-Sobecka, B., Boe-Hansen, R., Le Tallec, N., Waul, C.K., Arvin, E., 2011. A potential approach for monitoring drinking water quality from groundwater systems using organic matter fluorescence as an early warning for contamination events. *Water Research*, 45, 6030-6038.

Tang, J., Wu, K., 2012. Trend of Acid Rain Over China Since the 1990s. China Meteorological Administration. Source from http://www.esrl.noaa.gov/gmd/publications/annual_meetings/2013/abstracts/30-130408-C.pdf

Tang, J., Xu, X., Ba, J., Wang, S., 2010. Trends of the precipitation acidity over China during 1992–2006. *Chinese Science Bulletin*, 17, 1800-1807.

Tang, J., Xu, X.B., Yang, Z.B., Ba, J., Wang, S.F., 2008. The conductivity additivity of ionic components in precipitation and its application to the data evaluation of acid rain monitoring. *Journal of Applied Meteorological Science*, 19, 385-392. (In Chinese)

Thurman, E.M., 1985. *Organic Geochemistry of Natural waters*. Martinus Nijhof/Dr. W. Junk Publishers, Dordrecht, Boston, USA.

Tipping, E., Woof, C., 1991. The distribution of humic substances between the solid and aqueous phases of acid organic soils; a description based on humic heterogeneity and charge-dependent sorption equilibria. *Journal of Soil Science*, 42, 437-448.

Tipping, E., Woof, C., Rigg, E., Harrison, A.F., Ineson, P., Taylor, K., Benham, D., Poskitt, J., Rowland, A.P., Bol, R., Harkness, D.D., 1999. Climatic influences on the leaching of dissolved organic matter from upland UK

Moorland soils, investigated by a field manipulation experiment. *Environment International*, 25, 83-95.

Tissier, G., Perrette, Y., Dzikowski, M., Poulenard, J., Hobléa, F., Malet, E., Fanget, B., 2013. Seasonal changes of organic matter quality and quantity at the outlet of a forested karst system (La Roche Saint Alban, French Alps). *Journal of Hydrology*, 482, 139-148.

Toth, V.A., 1998. Spatial and temporal variations in the dissolved organic carbon concentrations in the vadose karst waters of MarenGo Cave Indiana. *Journal of Cave and Karst Studies*, 60, 167-171.

van Beynen, P., Ford, D., Schwarcz, H., 2000. Seasonal variability in organic substances in surface and cave waters at Marengo Cave, Indiana. *Hydrological Processes*, 14, 1177-1197.

van Beynen, P.E., Schwarcz, H.P., Ford, D.C., Timmins, G.T., 2002. Organic substances in cave drip waters: studies from Marengo Cave, Indiana. *Canadian Journal of Earth Sciences*, 39, 279-284.

Yang, Y., Saiers, James E., Xu, N., Minasian, S.G., Tyliszczak, T., Kozimor, S.A., Shuh, D.K., Barnett, M.O., 2012. Impact of natural organic matter on uranium transport through saturated geologic materials: from molecular to column scale. *Environmental Science & Technology*, 46, 5931-5938.

Yun, Y., Wang, H.M., Man, B.Y., Xiang, X., Zhou, J.P., Qiu, X., Duan, Y., Engel, A.S., 2016. The Relationship between pH and Bacterial Communities in a Single Karst Ecosystem and Its Implication for Soil Acidification. *Frontiers in Microbiology*, 7, 1955.

Zhang, W., Li, W.H., 2006. The temporal and spatial distribution of Water surface evapotranspiration in Yichang region. *Yangtze River*, 37, 30-31. (In Chinese)

Captions

Table 1 Summary data for annual (January to December) precipitation amount, annual mean air temperature, annual mean drip rates and annual mean fluorescence intensity (FI) and fluorescence wavelength maxima (FWM) values during the monitoring period. As a result of a rain gauge fault in June 2013 monthly rainfall data in June were lost. Rainfall amount in June 2013 was calculated with average rainfall amount (130.4 mm) in June from 2005 to 2012.

Figure 1. Location maps. study site shown as a yellow thumbtack. (a) pH of rainfall distribution in China, 2012 (Tang and Wu, 2012; modified); (b) relative position of Heshang Cave and four nearby acid rain monitoring stations (Yichang, Zigui, Jianshi and Wufeng); (c) Schematic diagram of Heshang karstic system showing the two drip sites of HS4 and HS6.

Figure 2. (a) Original emission fluorescence spectrum (excitation $\lambda = 320$ nm) of cave dripwaters (e.g. sample of 2009.06.08 from HS4 drip site) and blank water (deionized water); (b and c) aggregate emission fluorescence spectrum of all samples respectively from 350 to 500 nm after subtracting the background value of blank water. Shaded areas represent one standard deviation from the mean.

Figure 3. Monitoring data between 2004 and 2014 in Heshang Cave. (a) daily precipitation (data lost during June 2013 because of instrument breakdown); (b) monthly drip rate of HS4; (c and d) monthly fluorescence wavelength maxima and fluorescence intensity of dripwater of HS4; (samples of 2007.11.4 and 2010.9.19 missing); (e) monthly drip rate of HS6; (f and g) monthly fluorescence wavelength maxima and fluorescence intensity of dripwater of HS6 (samples of 2005.12.06 are missing); (i) monthly mean air temperature in Heshang Cave. Cyan

bars represent summer season (June to August), and blue horizontal dash lines represent baseflow values. n.d.=no data.

Figure 4. Sulphate concentration in local rainwater (grey circles) and corresponding predicted pH of local rainwater (red diamonds) from 2011 to 2015.

Figure 5. Daily (grey line), Monthly (grey hollow circles) and annual (black solid circles) volume-weighted pH of rainwater from Yichang acid rain station, compared with monthly (red hollow diamonds) and annual volume-weighted mean (red solid diamonds) predicted pH value of rainwater in Heshang region. Regression trendlines and correlation coefficient (R^2) are also shown respectively. The annual volume-weighted mean pH value in local rainwater of 2013 was not calculated due to 3 missing data points including rainfall amount and sulfate concentration in June, July and September respectively.

Figure 6. Rainfall/Drip rate and rainfall/fluorescence intensity cross-correlograms. k presents the lag time, $r(k)$ presents the correlation coefficient.

Figure 7. Relationships between annual precipitation amount (corrected by 734 mm, the annual mean evapotranspiration) and annual mean drip rate of HS4 and HS6.

Figure 8. Comparison of daily precipitation and monthly fluorescence intensity in dripwaters after eliminating a one year lag. Cyan bars represent the summer season (June to August).

Figure 9. Relationships between annual precipitation amount (corrected by 734 mm, the annual mean evapotranspiration) and fluorescence intensity. Black points (circles and diamonds) stand for the plot with a one year lag of fluorescence intensity, and pale points (circles and diamonds) stand for the plot without any lag.

Figure 10. Relationships between annual mean air temperature and fluorescence intensity with a one year lag of

fluorescence intensity.

Figure 11. Trends of annual precipitation amount, annual volume-weighted pH value of rainwater from Yichang acid rain station and annual mean fluorescence intensity of both dripwaters. (a) annual mean fluorescence intensity of HS4 from 2005 to 2013; (a) annual mean fluorescence intensity of HS6 from 2005 to 2013; (c) annual precipitation amount from 2004 to 2013; (d) annual volume-weighted pH value of rainwater from Yichang station from 2005 to 2015. Regression trendlines (Black lines) and correlation coefficient (R^2) are also shown.

Table 1

Year	Precipitation (mm)	Air temperature (°C)	Mean drip rate (ml/min)		Mean FWM (nm)		Mean FI at FWM (a.u.)	
					HS4	HS6	HS4	HS6
			HS4	HS6				
2004	1080	17.3						
2005	999	17.0	3.13	1.33	404.3	404.3	269.8	272.7
2006	816	18.4	2.10	0.95	403.4	403.6	220.2	231.3
2007	1247	17.5	3.07	1.57	404.9	405.8	220.3	246.2
2008	1354	17.1	3.40	1.72	405.2	406.2	274.3	316.8
2009	963	17.5	2.92	1.33	405.3	405.8	313.8	313.5
2010	987	17.2	2.70	1.28	405.4	404.5	201.0	223.2
2011	861	17.0	2.33	1.19	405.9	406.2	226.6	277.4
2012	771	16.4	1.89	1.20	406.0	405.0	209.3	222.4
2013	763	18.1	1.83	1.16	406.2	404.9	174.2	217.7
n's	10	10	9	9	9	9	9	9
Average	984	17.4	2.51	1.28	405.3	405.1	229.6	253.9

n's = number of cases; FWM = fluorescence wavelength maxima; FI = fluorescence intensity.

Figure 1

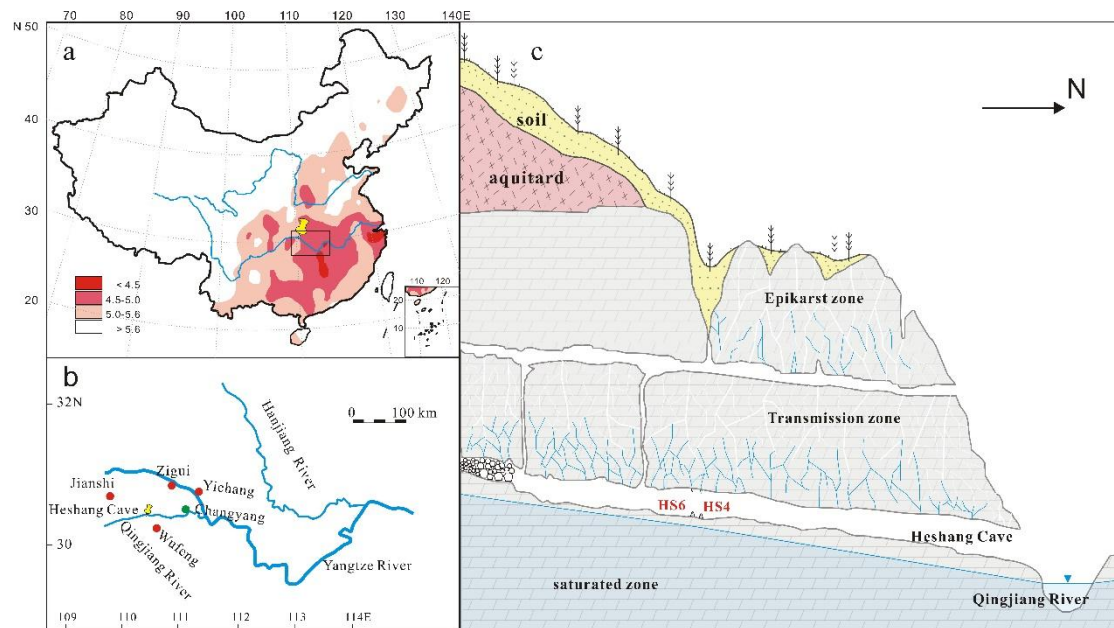


Figure 2

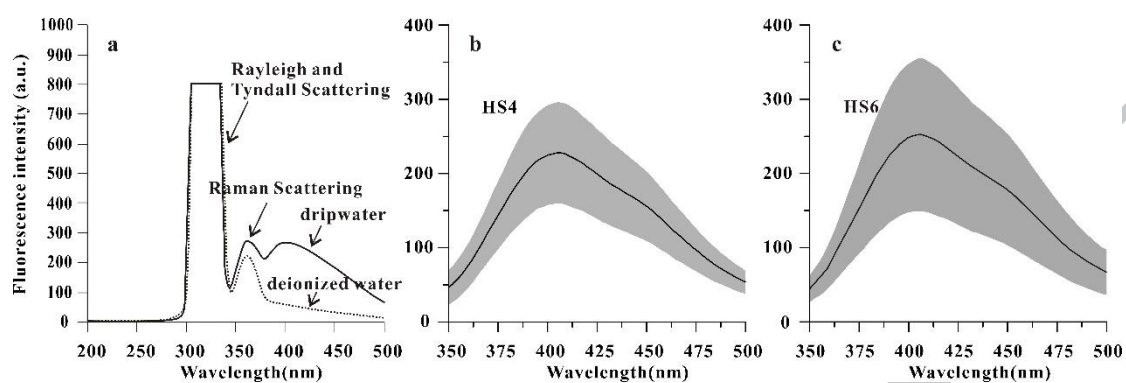


Figure 3

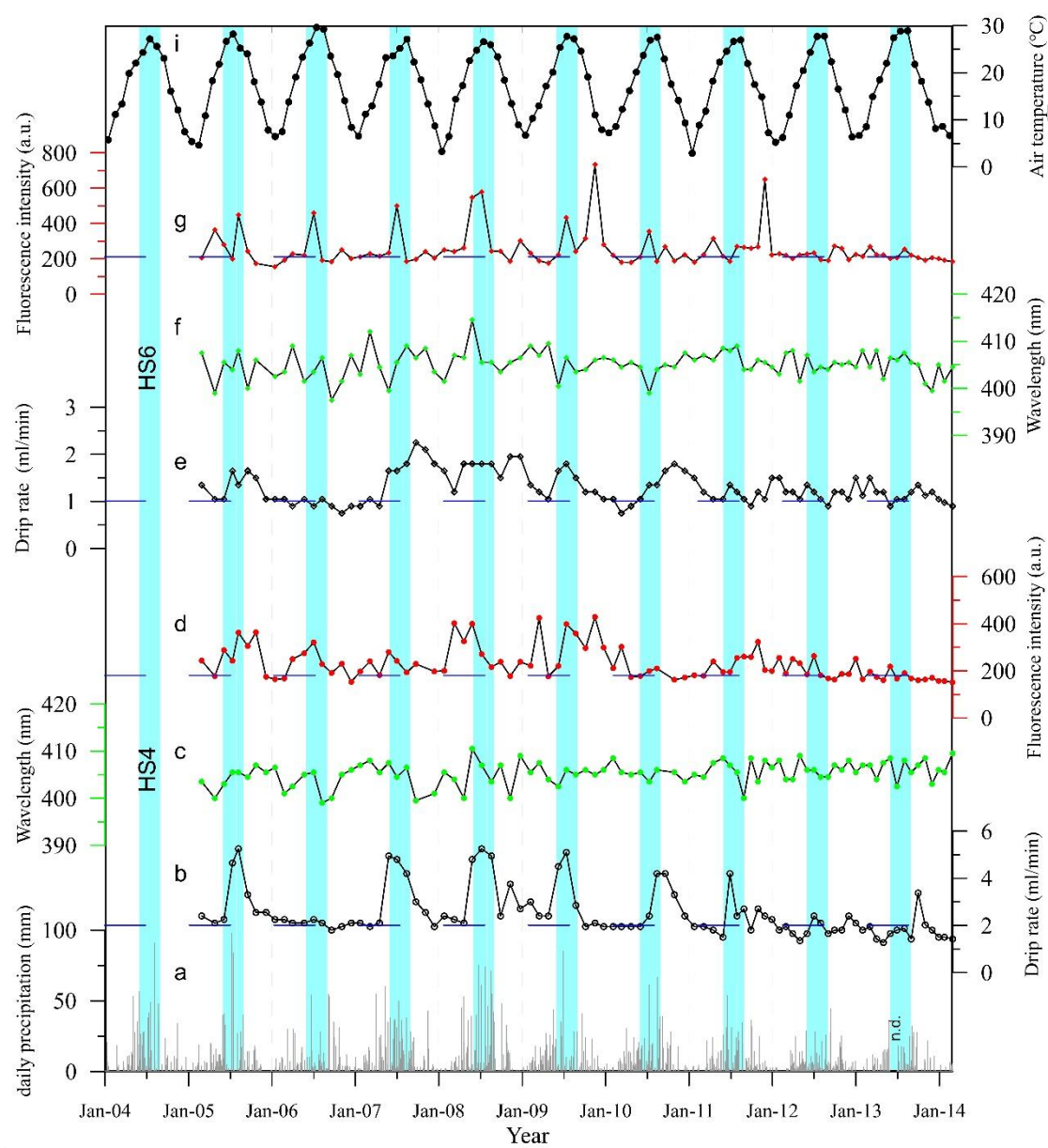


Figure 4

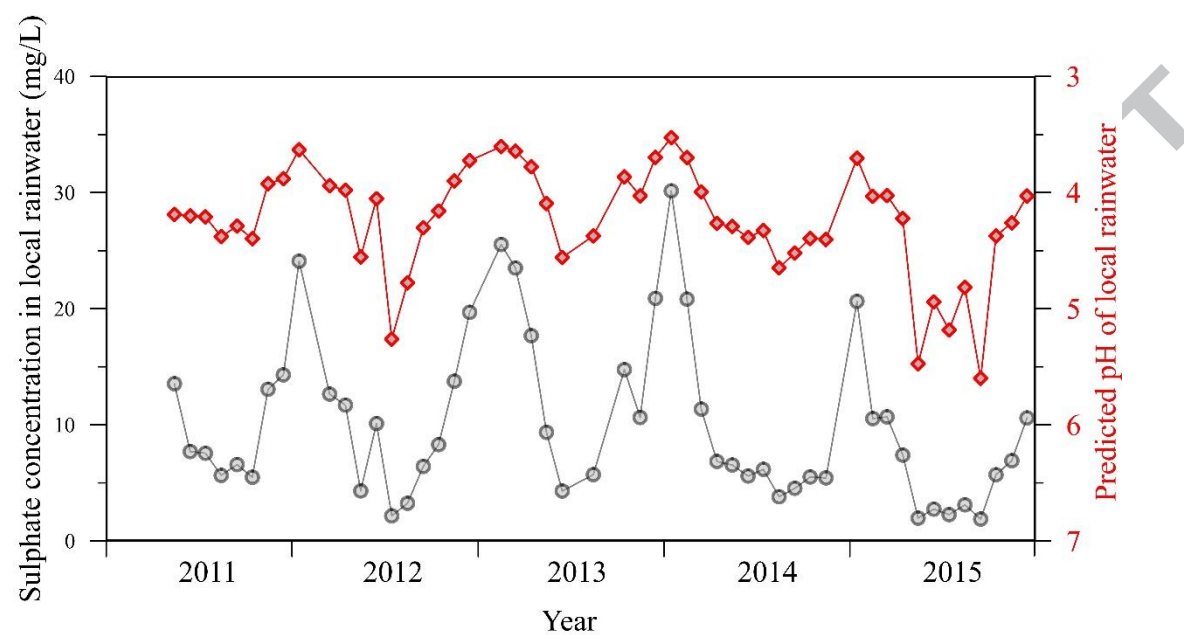


Figure 5

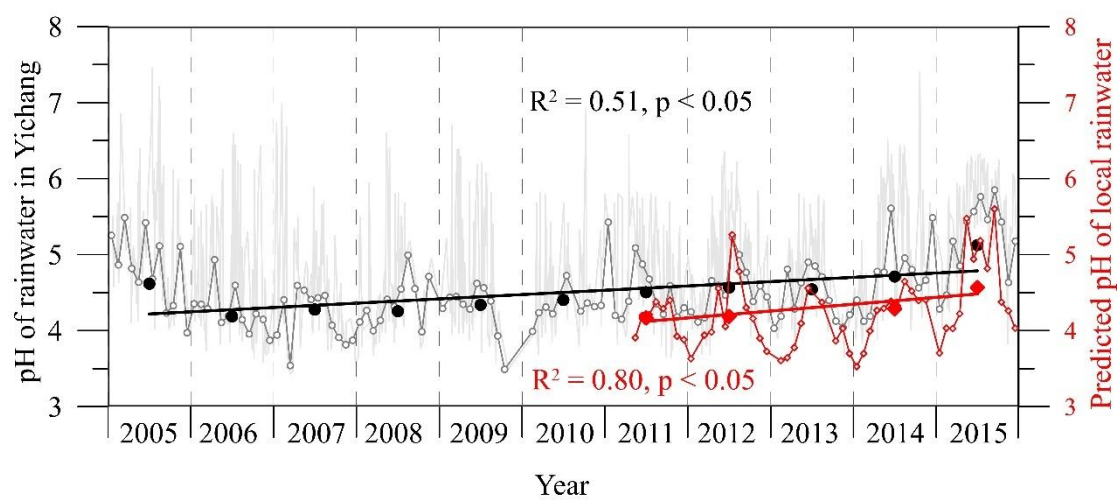


Figure 6

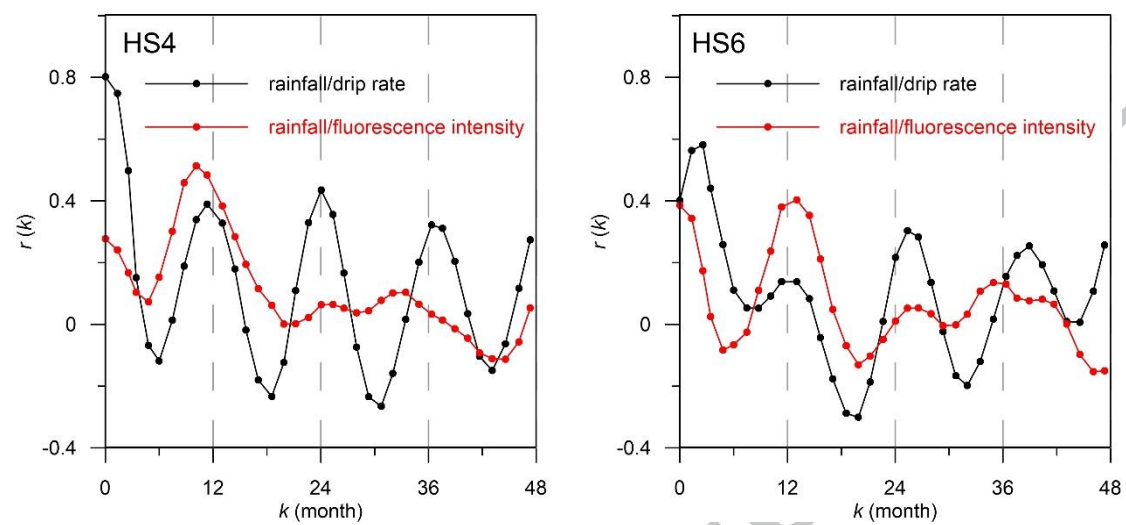


Figure 7

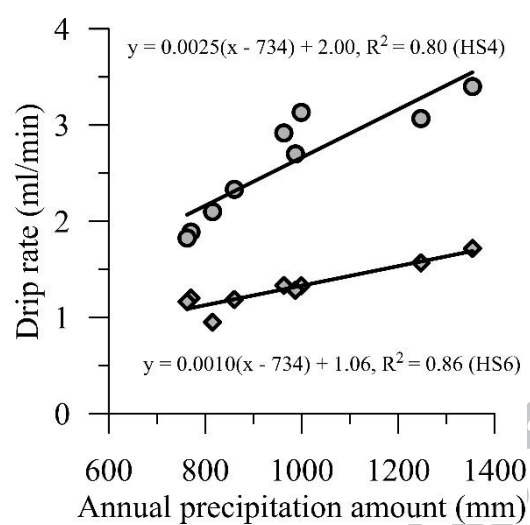


Figure 8

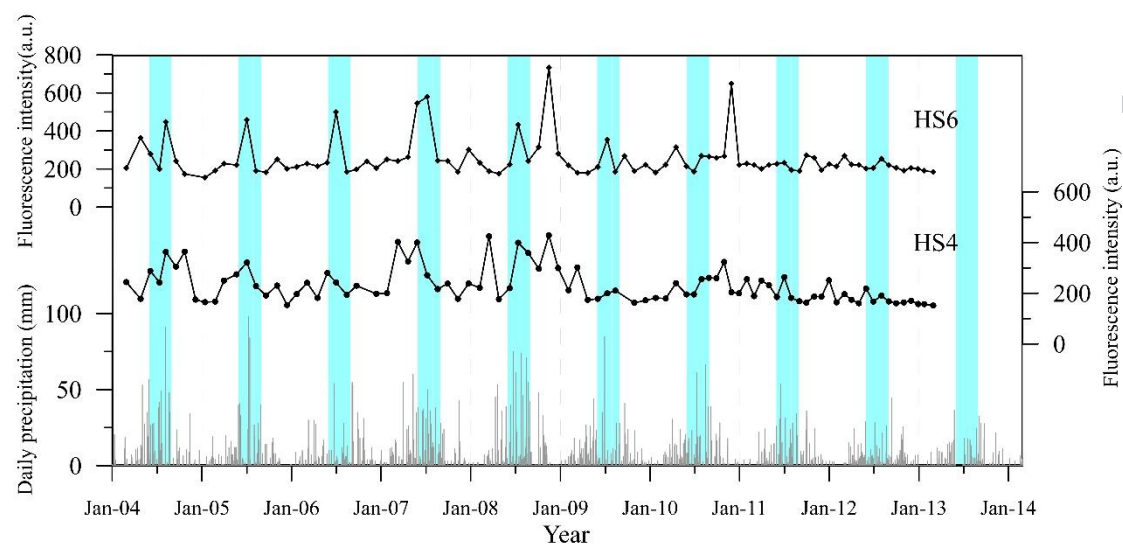


Figure 9

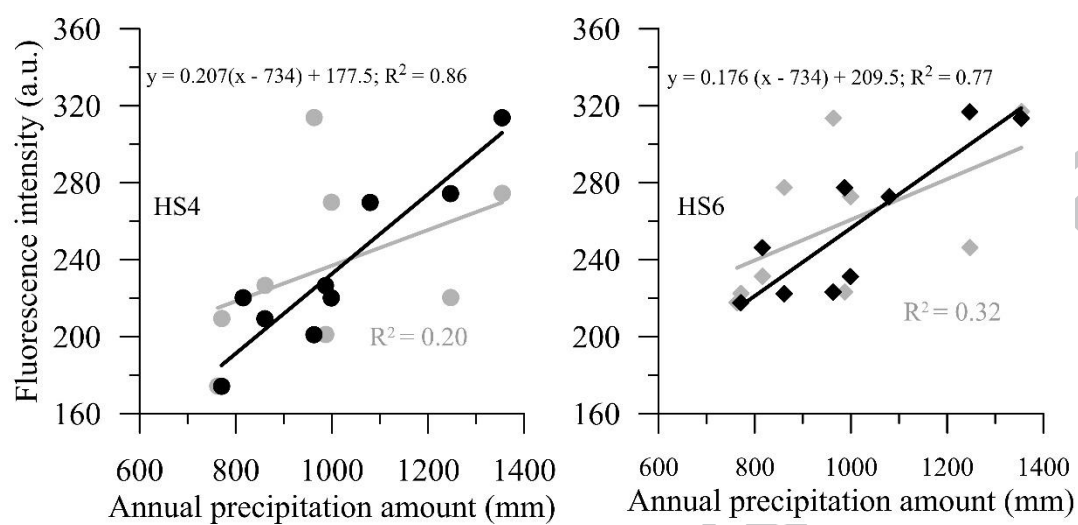


Figure 10

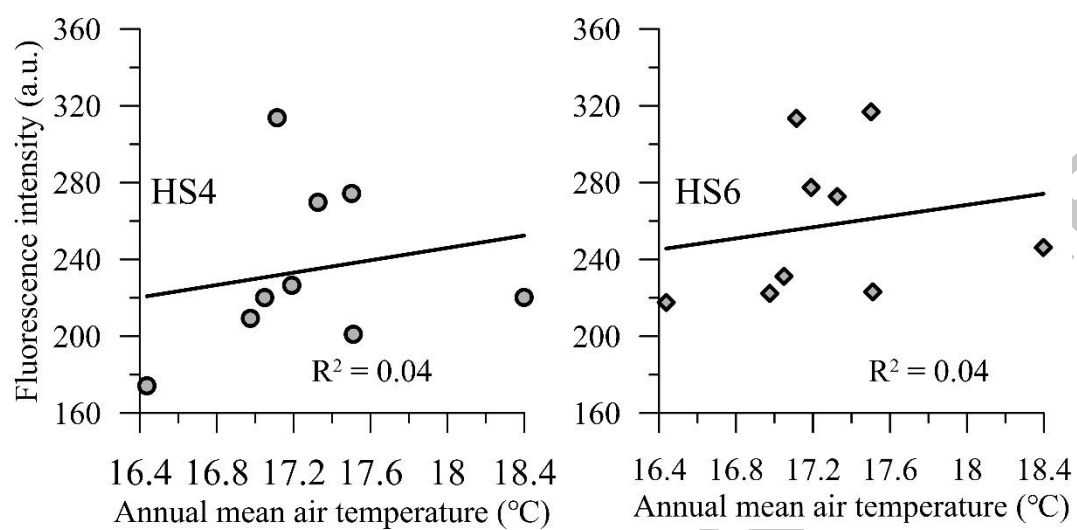
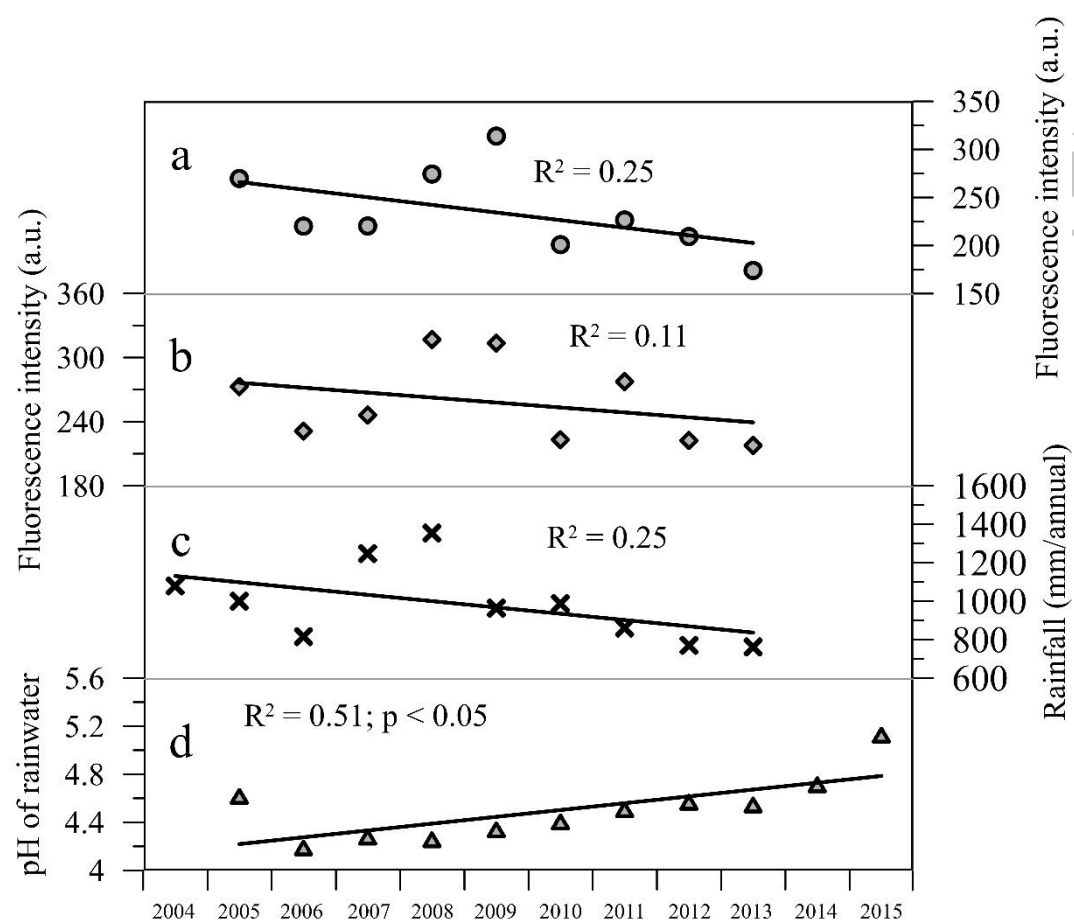


Figure 11



Highlights

1. The paper is the first comprehensive study on the effect of acid rain and climatic factors on dissolved organic matter variations in karst dripwaters over sub-annual to inter-annual time scale.
2. We report a continuous nine-year series of monthly dripwater fluorescence and discharge from two perennial drip sites.
3. The seasonality of fluorescence intensity mainly reflects the flushing of the soil zone and residence time of water governed by monsoonal rainfall; annual (effective) precipitation amount positively correlates with annual DOM concentration.
4. Current acid rain condition (~pH 5.6 to ~4.5) has no discernable effect on quality and quantity of DOM in karst systems, which strongly buffer acidification from atmospheric rainfall.